GU J Sci, Part A, 8(1): 81-93 (2021)

Gazi University

Journal of Science

PART A: ENGINEERING AND INNOVATION

http://dergipark.gov.tr/gujsa

Araştırma Makalesi Research Article

Modal Analysis of Horizontal Axis Wind Turbine Rotor Blade with Distinct Configurations under Aerodynamic Loading Cycle

Aniekan Essienubong IKPE[1*], Ekom Mike ETUK[2], Akanu-Ibiam Effiong NDON[3]

[1]*University of Benin, Department of Mechanical Engineering, Benin City, PMB 1154, Nigeria*
[2]*University of Benin, Department of Production Engineering, Benin City, PMB 1154, Nigeria*
[3]*Akwa Ibom State University, Department of Civil Engineering, Mkpat Enin, PMB 1167, Nigeria*

Keywords

Wind Turbine
Rotor Blade
Modal Analysis
Bending
Eigenfrequencies
Failure

Abstract

Q-Blade simulation tool was employed in modal analysis of horizontal axis wind turbine blade with three distinct configurations (with spar, no spar and solid) to determine the configuration with adequate structural integrity under aerodynamic loading conditions. The blade configurations were analysed in four different modes based on the flapwise and edgewise response of the blade to aerodynamic loads/forces, and the corresponding modal eigenfrequencies were evaluated. Bending due to combined effects of flapwise and edgewise modal frequencies on the blade were also evaluated at different rotor blade speeds ranging from 2-8m/s. It was observed that the solid blade configuration had the least modal eigenfrequencies for both flapwise and edgewise response in all the four modes as follows: 22.03 and 62.60 Hz in mode 1, 58.0 and 212.8 Hz in mode 2, 122.6 and 600.6 Hz in mode 3, 194.4 and 1118.9 Hz in mode 4. The rotor blade configuration with No spar had the highest modal eigenfrequencies for both flapwise and edgewise response in all the four modes followed by the blade configuration with spar. Bending of the rotor blade due to combined effects of flapwise and edgewise modal frequencies at the aforementioned blade speeds were also highest in blade configuration with No spar and lowest in the solid blade configuration. The low modal eigenfrequencies and low bending values on the solid blade configuration imply high stiffness and strength but with additional mass, which is why 6000 series aluminium was selected in order to minimize the extra weight.

Cite

Ikpe, A. E., Etuk, E. M., & Ndon, A. E. (2021). Modal Analysis of Horizontal Axis Wind Turbine Rotor Blade with Distinct Configurations under Aerodynamic Loading Cycle. *GU J Sci, Part A*, *8*(1), 81-93.

Author ID / (ORCID Number)

A. E. Ikpe, 0000-0001-9069-9676
E. M. Etuk, 0000-0002-1866-9349
A. E. Ndon, 0000-0002-2637-6546

Article Process

Submission Date 10.08.2020
Revision Date 20.12.2020
Accepted Date 04.03.2021
Published Date 29.03.2021

1. INTRODUCTION

Different number of blades is typically used in designing the horizontal axis wind turbines, depending on the purpose of the wind turbine. However, turbines with two or three blades are mostly used for power generation. Therefore, the most common designs of modern wind turbines are based on the horizontal shaft structure (Soriano et al., 2013). Upon approaching the wind turbine, there is a decline in wind speed and increase in wind turbulence. Consequently, rotation of the wind turbine blades result in turbulence, manifesting in the form of rotational vertical wakes (Etuk & Ikpe, 2020a).

The wind axis rotor blades during operation are subjected to structural loading conditions characterized by aerodynamic effects (velocity deficit, pressure differential, flow expansion, rotation of the wake field and increased turbulence) driving the wind/air particles in the atmosphere. The flow field around a wind turbine may be characterized by two major mechanisms such as convection and turbulent diffusion (Vermeer et al., 2003). Generally, wind turbine blades during operation may be subjected to lightning strikes, physical

*Corresponding Author, e-mail: aniekan.ikpe@eng.uniben.edu

impacts and damaging surface erosion conditions particularly in hostile terrains where the wind is accompanied by heavy rainfall (Yasuda et al., 2012; Garolera et al., 2016). Depending on severity of the aerodynamic forces which is a function of wind speed, the turbine rotor blades may be exposed to some degree of vibration which can be classified as forced vibration and resonant vibration. Forced vibration may occur due to external loads, internally generated forces/loads, unbalances and ambient excitation while resonant vibration is majorly caused by natural modes of vibration of the body (Brain & Mark, 1999).

An inherent property of any structure as related to vibration is the natural frequency of the structure. If a given structure vibrates at frequencies higher or closer to its natural frequency, the vibration may be exceptionally high (Ivan et al., 2014). It is therefore necessary to regularly evaluate the natural frequency of high load bearing structures such as the wind turbine blade to avoid unforeseen failure in service condition. The natural frequencies are thus said to be fundamental properties that are not dependent on the choice of coordinates. The mode shapes are often determined by finding the eigenvalues and the eigenvectors of the system. The operating deflection shape is defined as any forced motion of two or more points on the structure while the shape is defined by specifying the motion of two or more points, noting that motion is a vector quantity which signifies that it possesses magnitude and direction (Owunna et al., 2016).

Ikpe et al. (2018) reported that High Cycle Fatigue (HCF) due to repeated cyclic loading on rotor blades in service condition is a major cause of blade failure. Ikpe et al. (2019) employed three finite element solvers such as CATIA 2017 version, ANSYS R15.0 2017 version and HYPERMESH 2016 version in the modelling process of 0.40 mm x 0.40 mm plate. The corresponding mode shapes (Chladni patterns) as well as the modal frequencies were simulated using Finite Element Method (FEM). Result of modal frequency obtained from the experimental analysis agreed with the FEM simulated results, with HYPERMESH generated results being the closest to the experimental values. It was observed that the modal frequencies obtained from the FEM and experimental approach increased as the excitation time increased.

Finite element method (FEM) was employed by Efe-Ononeme et al. (2018) to determine the natural frequency of two turbine blade materials applicable to Trans-amadi power plant in Port Harcourt, Nigeria. Comparing the two gas turbine blade materials, the fundamental frequency under the same load conditions was 751 Hz for IN 738 and 896 Hz for U500 turbine blade material. This implies that the natural frequencies obtained for both materials were much higher than the operational frequency of 85Hz for resonance to occur. Therefore, resonance would be delayed across the blade materials in service condition, indicating that gas turbine blades designed with both materials would be dynamically stable under operational frequency approaching 745 Hz.

Etuk et al. (2020b) investigated the normal, radial, axial and tangential loading cycles undergone by wind turbine rotor blades and their effects on the displacement of the blade structure using QBlade finite element sub module. Geometry of the deformed blades were characterized by twisting and bending configuration at maximum strain deformation at frequencies up to 200 Hz. From the deflection values obtained, it was found that normal loading cycle would cause the highest level of structural damage on the rotor blade followed by radial, axial and tangential loading. To increase the reliability of a wind turbine blade, Mouhsine et al. (2018) developed an airfoil structure to calculate the optimum blade geometry for the procedure. The optimum efficient geometry was complex, consisting of airfoils sections of increasing width, thickness and twist angle towards the hub. At a nominal wind speed of 12 m/s, 0.045 m was obtained as the tip displacement of the blade.

Studies have shown that turbine rotor blades in recent times are manufactured from composite materials because, they satisfy complex design constraints such as light weight and high stiffness while also providing adequate resistance to the static and aerodynamic loads (Bagherpoora & Xuemin, 2017). The failure analysis of two sandwich composite wind turbine rotor blade with 1 and 2.5m length subjected to wind load was carried out by Chen & Kam (2011), through theoretical and experimental approaches. The skin and core of the turbine blade were made of Glass fabre/epoxy composite laminae and PVC foam while the handle at the blade root was made of aluminium alloy. Stresses in the turbine blade were determined through finite element code ANSYS while the skin and the core of the blade were modelled using shell and solid

elements. A phenomenological failure criterion was employed in predicting the first-ply failure strength of the blade. The measured ultimate load of the rotor blade was used to validate the results which was found to be accurate in predicting fairly good ultimate failure load and failure location of 1m long when compared to the experimental results.

Okokpujie et al. (2020) implemented a multi-criteria decision method (MCDM) to select the best material for developing a horizontal wind turbine blade, considering aluminium alloy, stainless steel, glass fibre, and mild steel as alternative materials. Quantitative research approach using AHP and TOPSIS multi-criteria decision method was employed. The result revealed a consistency index of 0.056 and a consistency ratio of 0.062 obtained via the AHP method. 78%, 43%, 67%, and 25% were the performance scores, and aluminium alloy was selected as the best material, followed by glass fibre.

Operational modal analysis to extract the modal parameters before failure and operational modal analysis on the damaged structure of the 6.4 m length turbine blade made of glass fibres combined with epoxy resin was conducted by Marulo et al. (2014). The Experimental results revealed a decrease in the natural frequencies and an increase of the estimated modal damping of the structure. The reduction in natural frequencies was due to decrease in the stiffness of the structure. Results of the operational modal analysis were compared with numerical ones and correlation was found between them. Hence, it was concluded that structural integrity of a structure can be monitored by using modal parameters, like natural frequencies, damping characteristics and mode shapes.

Pedersen & Kristensen (2003) compared the results from two experiments, i.e. frequency, damping and the mode shapes. The orientation of the blade some effects on the measured results obtained by modal analysis. There were variations in the measured frequency up to 1.6% at 1 edgewise and 3 flapwise natural frequencies. The damping results had variations up to 56%, at 3 flapwise natural frequency. The uncertainty on the damping was due to smaller quantities of the damping characteristics.

A comparative study was conducted by Taware et al. (2016), using Glass Fibre Reinforced Plastic (GFRP) blade and GFRP blade with steel wire mesh to determine the natural frequencies and deformation of mode shape. It was observed that natural frequencies for the first three modes of the GFRP blade with steel mesh increased by 2-3% more than only the GFRP blade. Also, the mode shapes for the first three modes indicated that there was less variation in deformation of the GFRP blade than the GFRP blade with steel wire mesh. The obtained natural frequencies gave the resonant condition frequencies for both blades.

In this study, modal analysis of horizontal axis wind rotor blade with distinct configurations was carried to determine the structural integrity of each blade configuration under aerodynamic loading conditions.

2. MATERIAL AND METHOD

Wind turbine blades are composed of two faces (the suction face and the pressure face), bound together and stiffened either by one or more integral (shear) webs connecting the upper and lower section of the blade shell or by a box beam (box spar with shell fairings) (Brøndsted & Nijssen, 2013). The shells are adhesively joined together to the spars. The flapwise load is as a result of the wind pressure while the edgewise load is due to gravitational forces and torque load acting on the blade. The flapwise bending is resisted by the spar, internal webs or spar inside the blade, while the edges of the profile carry the edgewise bending. From the loading points on material, one of the main laminates in the main spar is subjected to cyclic tension-tension loads (pressure side) while the other (suction side) is subjected to cyclic compression-compression loads. The laminates at the leading and trailing edges that carry the bending moments related to the gravitation loads are subjected to tension-compression loads (Mishnaevsky et al., 2017). Figure 1 represents detailed illustration of the rotor blade section. QBlade is a Blade Element Moment Method (BEM), Double Multiple Streamtube (DMS) and nonlinear lifting line theory (LLT) design and simulation software for vertical and horizontal axis wind turbine. QBlade incorporates a number of tools such as QFEM to setup and simulate the internal blade structure and perform structural blade design, modal analysis, static deflection as well as stress analysis.

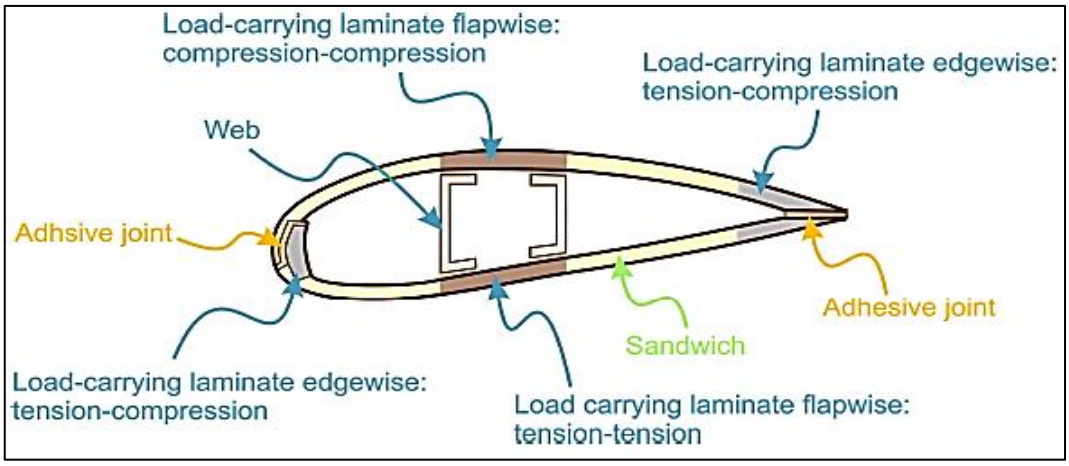

Figure 1. *Illustration of the Rotor Blade Section*

In this study, QBlade v0.8 was employed in the modal analysis of different blade configurations using the isotropic tapered Euler Beam elements in order to evaluate the modal eigenfrequencies and associated bending effects to determine the most suitable blade configuration that can withstand structural failure due to aerodynamic loads/forces from the wind and the bending stresses resulting thereof. The respective chord lengths and angle of twist of each section is shown in Figure 2. The total length of the blade was 2.2 m, total number of sections was 15 while the number of blades employed in the simulation process was 3. The blade was divided into 15 sections. The first three sections had the circular foil applied at the blade section while the remaining 12 sections had NACA 4610 airfoil applied on them. The blade geometry/root coordinates is presented in Figure 2.

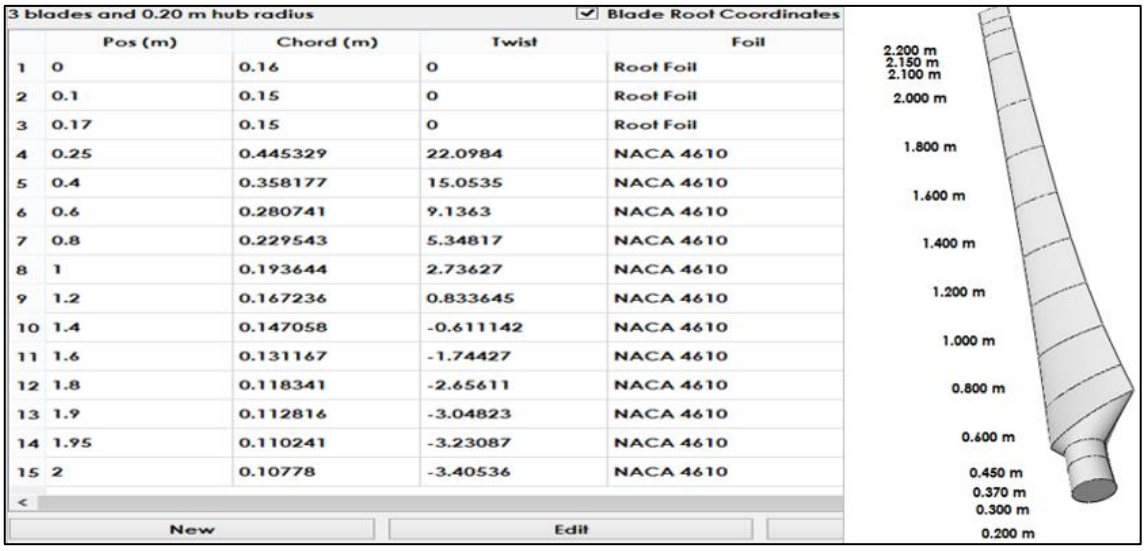
3 blades and 0.20 m hub radius — Blade Root Coordinates

	Pos (m)	Chord (m)	Twist	Foil
1	0	0.16	0	Root Foil
2	0.1	0.15	0	Root Foil
3	0.17	0.15	0	Root Foil
4	0.25	0.445329	22.0984	NACA 4610
5	0.4	0.358177	15.0535	NACA 4610
6	0.6	0.280741	9.1363	NACA 4610
7	0.8	0.229543	5.34817	NACA 4610
8	1	0.193644	2.73627	NACA 4610
9	1.2	0.167236	0.833645	NACA 4610
10	1.4	0.147058	-0.611142	NACA 4610
11	1.6	0.131167	-1.74427	NACA 4610
12	1.8	0.118341	-2.65611	NACA 4610
13	1.9	0.112816	-3.04823	NACA 4610
14	1.95	0.110241	-3.23087	NACA 4610
15	2	0.10778	-3.40536	NACA 4610

New Edit

Figure 2. *Blade Geometry/Root Coordinates*

Loading data was imported from a previously simulated turbine that uses the same rotor. In the structural blade design module, a simple structural model was defined for the rotor blade inside the Structural Blade Design/Modal Analysis tab. The model was defined and simulated using isotropic material properties only. After defining the structural model, sectional blade properties were computed and a modal analysis had been performed. The resulting mode shapes and frequencies were visualized and changed from the dock window. At this stage, the structural properties can be plotted in graphs, by changing to Graph View in the toolbar. This study was carried out using three horizontal wind turbine blade configurations such as hollow with spar, hollow without spar and the solid configuration. Properties of the rotor blade analyzed in this study are presented in Table 1. Longer blades are prone to high deflections, making structural stiffness (to ensure tip clearance, i.e., to avoid the blade from hitting the tower) a significant factor in the blade design, but stiffness-to-weight ratio is of major importance from the material perspective (Ikpe et al., 2016a,

2016b). The various frequency eigenmodes are to determine structural integrity of the rotor blade under aerodynamic loading conditions. The three blade configurations employed in this study are presented in Figure 3.

Table 1. *Material Properties of the 6000 Series Aluminium Rotor Blade*

Properties	Shell Material specifications	Internal Material specifications
	6000 Series Aluminium	Polyurethane 20GF 6SD
Density (kg/m^3)	2740	1360
Elastic Modulus (MPa)	7e+04	1.72e+03
Mass (kg)	Hollow with Spar:13.2465 Hollow no Spar: 12.1003 solid: 31.535	
Section No.	Rotational Speed	119(1/min)
	Shell Thickness (m)	Spar Thickness (m)
1	0.00320	0.01280
2	0.0030	0.01200
3	0.0030	0.01200
4	0.00961	0.03844
5	0.00773	0.03092
6	0.00606	0.02423
7	0.00495	0.01981
8	0.00418	0.01671
9	0.00361	0.01444
10	0.00317	0.01269
11	0.00283	0.01132
12	0.00255	0.01021
13	0.00243	0.00974
14	0.00238	0.00952
15	0.00233	0.00930

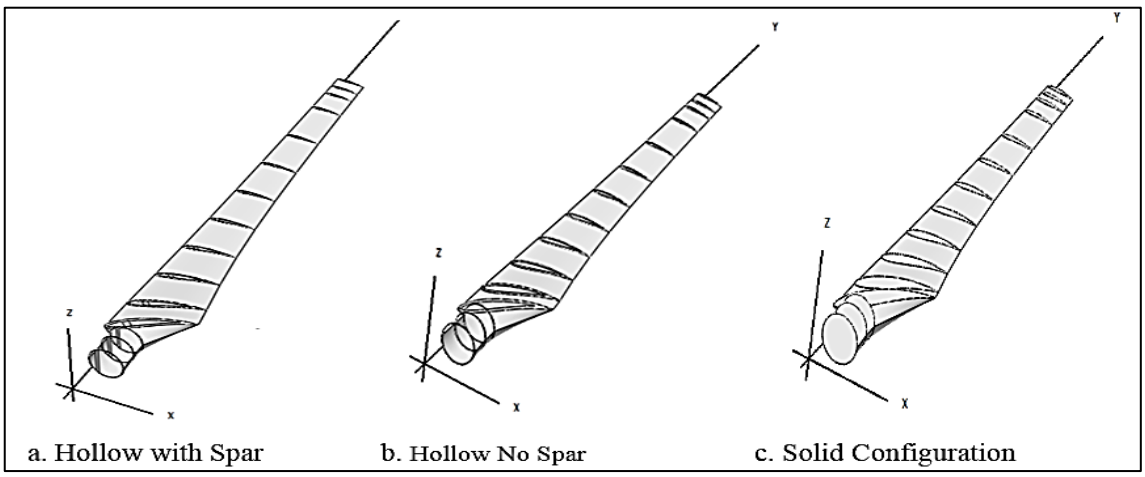

Figure 3. *The Three Blade Configurations Employed in This Study*

Figure 3 represents typical rotor blade configurations for horizontal wind turbine application. It can be observed in the above rotor blade configurations that some of the blades are configured with a hollow pattern reinforced with spar (see Figure 3a), some of them are configured with just a hollow pattern with no spar (see Figure 3b) while some of them are configured without spar and hollow pattern (see Figure 3c). The hollow pattern is simply a configuration in which a center hole or trench is made at the mid-section of the blade. This is sometimes applicable to high density rotor blades where the mid-section are made hollow

in order to reduce the blade density. In such case, the trench can extend fully or partially along the blade length (i.e., span-wise direction).

The term "spar" is a beam-like structural member that supports the ribs in an airfoil, aircraft wing or wind rotor blades, and running span-wise at right angles to the blade leading edge. In other words, spars which serves as a reinforcing members of a wind turbine rotor blade increases the structural strength and stiffness of the blade to prevent tower strikes in the event of sudden wind gusts, forms the structural framework upon which reduction in axial fatigue, improvement of compressive strain, buckling resistance as well as resistance to gravitational and aerodynamic loads are well assured. Spars are usually "L or T" shaped member installed within the hollow section of the rotor blade. It consist of upper and lower members known as spar caps and vertical sheet members known as shear webs which spans the distance between the spar caps of which the spar caps are welded or riveted to the top and bottom of the vertical member to prevent buckling.

The third rotor blade configuration as shown in Figure 3c is the solid configuration which neither has spars nor hole in the mid-section of the blade. The solid blade in this case is densely rigid with no internal holds, solid in cross section with both interior and exterior part uniformly filled with the same material. Like every other rotor blades, the leading and trailing edges are properly streamlined to meet aerodynamic specifications for wind turbine rotor blades.

3. RESULTS AND DISCUSSION

When the direction of wind flows along a cambered airfoil/wind rotor blade which has some degree of curvature, the wind velocity and acceleration continues to change along the blade radius, producing aerodynamic forces that acts on the blade as the wind speed changes. Different force components were observed at different sections of the curved blade. One of the force components is normal to the tangent or towards the center of curvature of the rotor blade. This component is known as normal force which is acting at that point. Normal loading or forces are those forces acting perpendicularly to the direction of motion. In other words, normal component of force does not change the magnitude of the flow velocity but changes the direction of velocity at that point. Values obtained for normal loads and tangential loads acting along the turbine rotor blade sections at wind speeds ranging from 2-8 m/s are presented in Table 2.

Table 2. *Normal and Tangential Loads Along Blade Sections at Different Wind Speeds*

Blade Radius (m)	Normal Loading at different Wind speeds				Tangential Loading at different Wind speeds			
	2m/s	4m/s	6m/s	8m/s	2m/s	4m/s	6m/s	8m/s
0.00	0.44	1.30	2.66	4.53	-0.86	-1.43	-2.29	-3.40
0.10	0.62	1.71	3.39	5.68	-1.32	-1.88	-2.70	-3.74
0.17	1.16	2.79	4.44	6.84	-1.94	-2.17	-3.11	-4.42
0.25	1.06	8.47	19.14	32.19	-0.33	2.83	9.02	19.57
0.40	2.00	11.90	26.39	42.93	0.35	3.92	11.99	24.72
0.60	3.69	15.98	32.56	44.06	0.41	3.91	12.55	20.39
0.80	5.69	20.43	38.45	42.61	0.34	3.78	12.70	14.48
1.00	8.25	25.21	44.27	43.99	0.21	3.63	12.58	12.14
1.20	11.58	30.23	49.97	48.10	0.06	3.50	12.33	12.18
1.40	15.34	35.13	55.28	53.77	-0.10	3.36	11.96	13.31
1.60	19.59	40.02	60.00	61.05	-0.29	3.19	11.23	14.90
1.80	23.56	43.54	62.57	68.41	-0.45	2.87	9.82	15.61
1.90	24.75	41.92	58.32	67.77	-0.43	2.43	7.42	13.97
1.95	26.61	33.83	47.75	57.61	-0.32	1.93	5.42	10.76
2.20	8.47	18.15	26.76	32.56	0.17	1.12	2.95	5.49

The other component of force is in the direction tangential to the blade at a given point. This component is known as the tangential force acting at that point. Tangential loading or forces are those forces acting along the direction of motion. In other words, the said tangential force does not change the direction of motion but changes the velocity magnitude. Values obtained for tangential loads/forces acting along the turbine rotor blade sections at different wind speeds are presented in Table 2. Table 3 indicates radial and axial loads/forces acting along the blade sections at different wind speeds. Etuk et al. (2020b) classified the loading conditions as normal load due to vibration of the rotor blade, axial load due to wake loses, tangential load or point load on different sections of the blade due to wind direction and radial load due to cyclic motion of the blade within the wind field domain. Table 2 and 3 indicates that the loading cycles increase as the blade radius increases. This is because the trailing edge of the blade towards the tip becomes slender and more streamlined against drag and wake forces. This in turn serves as advantage to the rotor which then rotates with increased speed, but at higher loading cycle in attempt to overcome the associated aerodynamic loads in the wind field domain.

Table 3. *Normal and Tangential Loading Along Blade Sections at Different Wind Speeds*

Blade Radius (m)	Radial Loading at different Wind speeds				Axial Loading at different Wind speeds			
	2m/s	4m/s	6m/s	8m/s	2m/s	4m/s	6m/s	8m/s
0.00	0.40	1.24	2.31	3.34	-0.62	-1.34	-2.03	-3.24
0.10	0.56	1.62	3.02	4.28	-1.14	-1.63	-2.30	-3.42
0.17	1.12	2.50	3.54	5.72	-1.53	-2.02	-2.58	-4.26
0.25	1.04	7.45	17.17	26.16	-0.28	2.19	7.21	17.73
0.40	1.08	10.52	24.28	37.42	0.30	2.29	9.32	22.12
0.60	2.46	13.18	28.16	40.26	0.38	2.41	11.15	18.36
0.80	4.52	18.47	33.35	38.61	0.28	2.56	11.34	13.85
1.00	6.25	23.30	38.37	39.99	0.19	2.64	11.50	12.10
1.20	8.53	28.24	42.63	44.80	0.03	2.58	11.16	12.15
1.40	12.24	31.12	48.18	47.27	-0.07	3.22	10.52	13.02
1.60	15.45	34.06	54.40	53.62	-0.24	3.03	10.19	14.20
1.80	17.61	39.14	57.62	58.54	-0.41	2.52	8.12	13.61
1.90	20.87	35.92	61.26	62.31	-0.39	2.24	6.75	11.97
1.95	23.36	29.72	40.27	52.11	-0.28	1.64	3.52	8.76
2.00	6.84	16.08	23.40	47.58	0.14	1.06	2.10	3.49

3.1. Modal Analysis Results

Result obtained for the modal analysis is a representation of how the blade will response to aerodynamic loads (see Table 2 and 3) in the flapwise and edgewise direction. Flapwise response of the rotor blade shows the blade response along the z-axis or deflection of the blade towards the blade flap, which is at the surface along the trailing edge. However, edgewise response of the rotor blade indicates response along the x-axis or deflection towards the edges of the rotor blade. In other words, aerodynamic forces/loads are parallel to the rotor edges for the edgewise deflection and perpendicular to the local chord or rotor plane for the flapwise deflection. eigenfrequency also known as natural frequency is a certain discrete frequency at which the rotor blade tends to vibrate (Bhatt, 2009). When vibrating at certain eigenfrequency, the rotor blade deforms into a corresponding shape known as eigenmodes. According to Larsen et al. (2002), modes are inherent properties of a given structure, and are determined by the properties of the material (density, stiffness, and damping behaviour) and boundary conditions of such structure. Each mode is characterized mainly by natural frequency, modal damping and mode shapes also known as modal parameters. As shown in Figure 4a-7a, eigenfrequency analysis only provides the shape of the mode not the amplitude of any physical vibration of the rotor blade (Higham et al., 2008). Figure 4b-7b represents the plots for flapwise eigenfrequency and edgewise eigenfrequency for the three (3) blade configuration considered in this study.

The solid blade has the lowest eigenfrequency values of 22.03 Hz at flapwise direction and 62.60 Hz at edgewise direction for mode 1, compared to the hollow blade configuration with no spar which has the highest eigenfrequency values followed by hollow blade configuration with spar. Deformation of modal shape in mode 1 is barely observed for flapwise deflection and observed at the mid-span of the blade for edgewise deflection, causing slight bending on the mode shape as shown in Figure 4a.

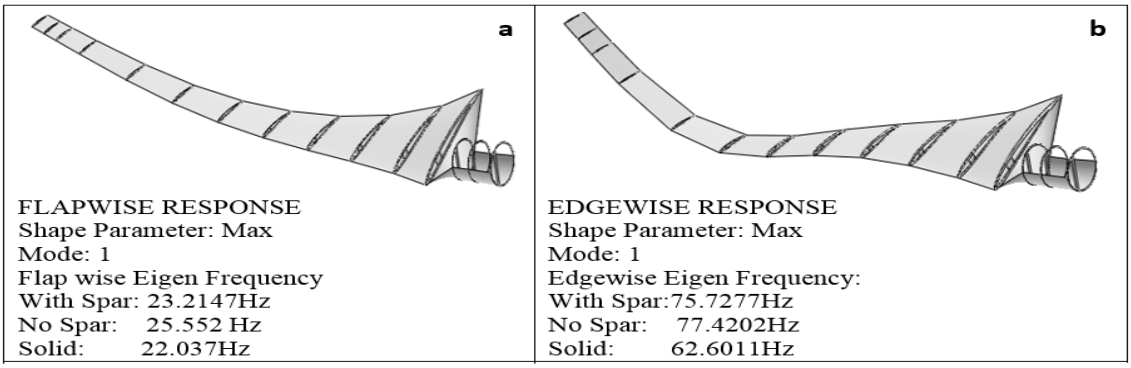

Figure 4a. *Flapwise and Edgewise Response of Rotor Blade Modal Shape 1*

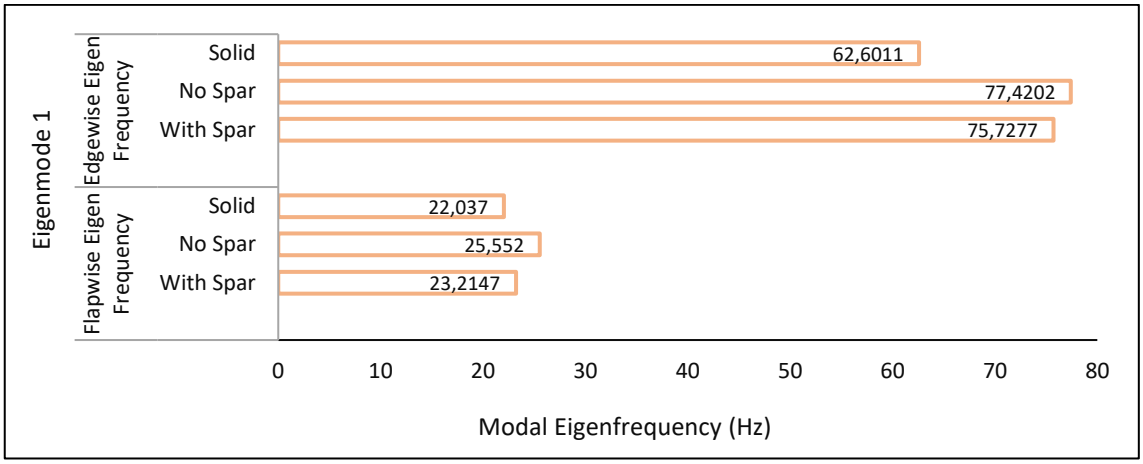

Figure 4b. *Corresponding Modal Eigenfrequencies for Modal Shape 1*

Similarly in mode 2, the solid blade has the lowest eigenfrequency value of 58.0 Hz at flapwise direction and 212.8 Hz at edgewise direction compared to the hollow blade configuration with no spar which has the highest eigenfrequency values followed by hollow blade configuration with spar. The blade response to aerodynamic loads (see Table 2 and 3) in mode 2 is observed at the mid-span of the blade for the flapwise deflection and observed to extend from the mid-span of the blade to the blade for the edgewise deflection, causing significant bending on the mode shape as shown in Figure 5a.

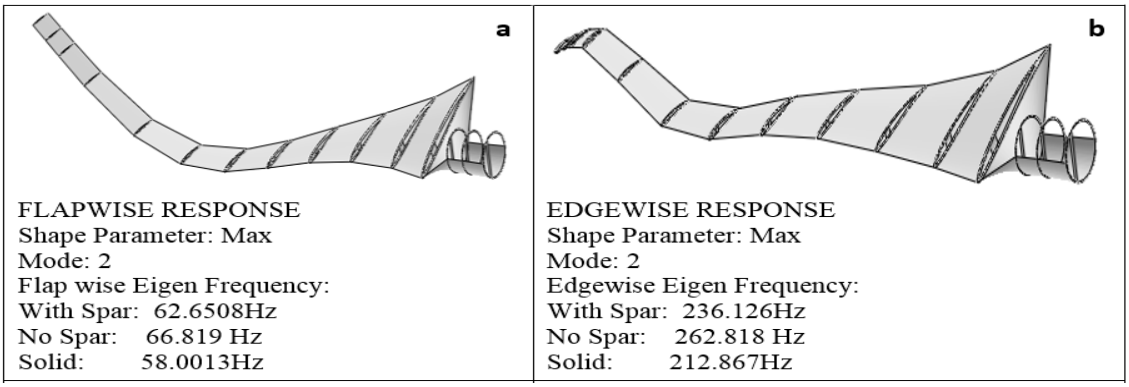

Figure 5a. *Flapwise and Edgewise Response of Rotor Blade Modal Shape 2*

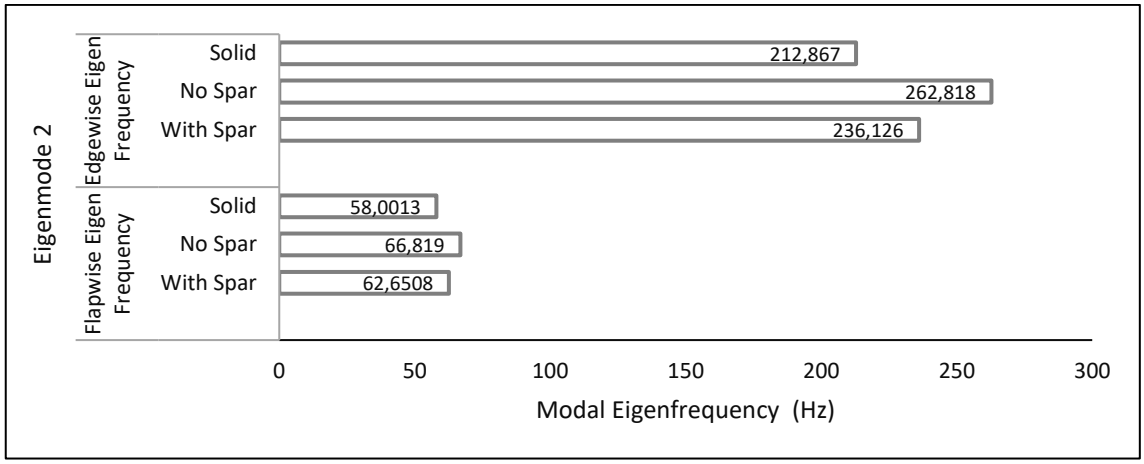

Figure 5b. *Corresponding Modal Eigenfrequencies for Modal Shape 2*

In mode 3, the solid blade has the lowest eigenfrequency values of 122.6 Hz at flapwise direction and 600.6 Hz at edgewise direction compared to the hollow blade configuration with no spar which has the highest eigenfrequency values followed by hollow blade configuration with spar. The blade response to aerodynamic loads (see Table 2 and 3) in mode 3 is observed to extend from the mid-span of the blade to the trailing edge for the flapwise deflection and observed to extend from the mid-span of the blade to the blade tip and slightly to the blade leading edge for edgewise deflection, causing significant deformation and distortion on the blade modal shape as shown in Figure 6a.

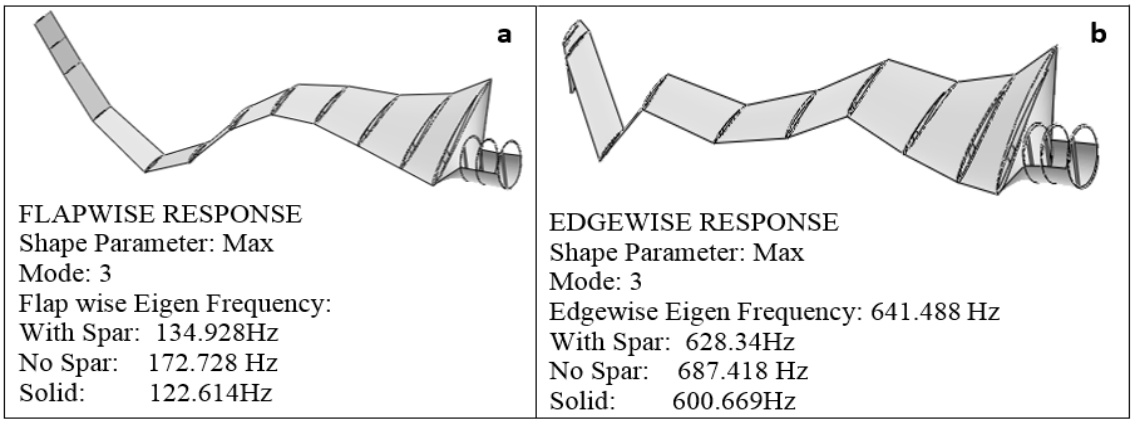

Figure 6a. *Flapwise and Edgewise Response of Rotor Blade Modal Shape 3*

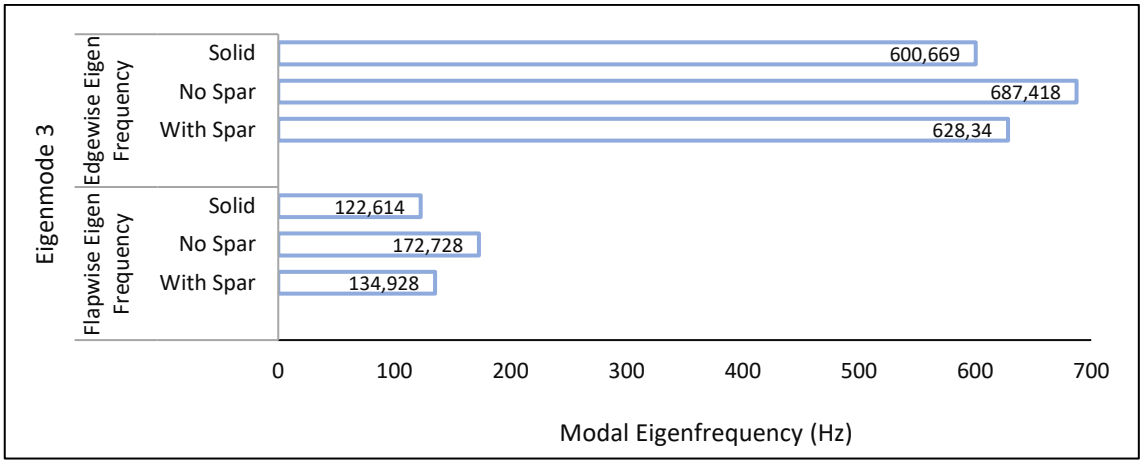

Figure 6b. *Corresponding Modal Eigenfrequencies for Modal Shape 3*

Finally in mode 4, solid blade configuration also has the lowest eigenfrequency values of 194.4 Hz at flapwise direction and 1118.9 Hz at edgewise direction compared to the hollow blade configuration with

no spar which has the highest eigenfrequency values followed by hollow blade configuration with spar. The blade response to aerodynamic loads (see Table 2 and 3) in mode 4 caused damage from the mid-span, across the trailing edge of the blade and towards the blade tip for flapwise response. The blade was observed to deflect towards the tip. For edgewise response, the aerodynamic loads were observed to affect the entire blade except for some parts between the leading edge and the blade root, causing significant deformation and distortion on the blade characterised by twisting modal shape as shown in Figure 7a.

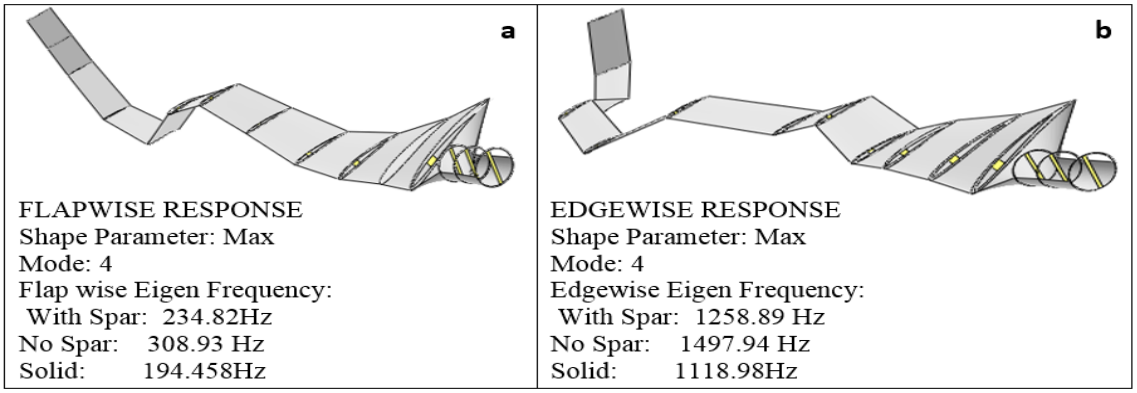

Figure 7a. *Flapwise and Edgewise Response of Rotor Blade Modal Shape 4*

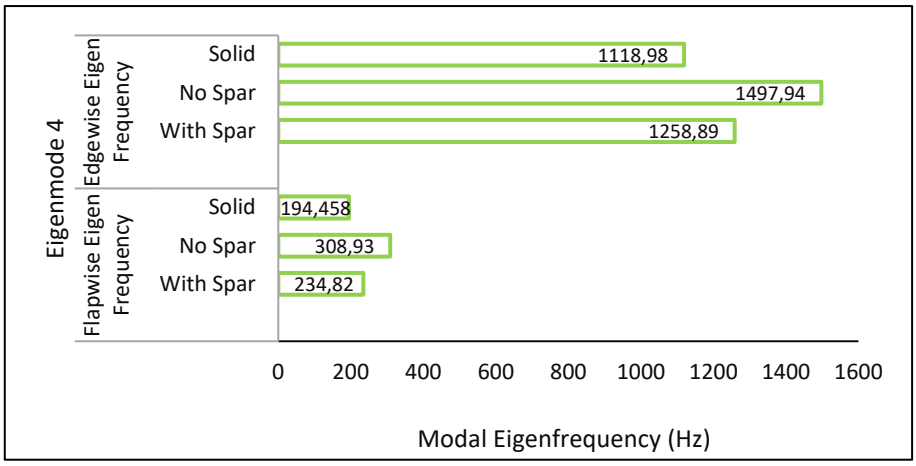

Figure 7b. *Corresponding Modal Eigenfrequencies for Modal Shape 4*

Figure 8-11 represents bending on the turbine rotor blade for different eigenmodes ranging from 1-4 at various wind speeds ranging from 2-8m/s. The bending values plotted for each eigenmodes indicate that the eigenmodes are characterised by different modal frequencies and rotational speeds resulting in bending effects of the blade. The bending effect is as a result of natural frequencies at each revolution speed of the blade which is at increasing order. Modal analysis carried out by Chaudhari (2014) on horizontal wind turbine blade at rotational speeds of 5 and 10m/min revealed that natural frequency of the turbine blade increases as the rotor speed also increase. On the other hand, Tartibu et al. (2012) in their investigation found that the blade natural frequency increased as the eigenmodes progressed. It can be observed in Figures 8-11 that bending due to the combined effects of natural frequency or modal eigenfrequency at the flapwise and edgewise direction of the rotor blade increased correspondingly with increase in the eigenmodes and rotor blade speeds. This in turn resulted in the bending effects on the blade which increased gradually as the rotor speeds and its eigenmodes increased. It should be noted that each mode is defined by a natural (modal or resonant) frequency, modal damping and a mode shape. As represented on each plot in Figures 8-11, the highest bending effect on each configuration of the blade at various rotor speeds (2, 4, 6 and 8m/s) considered in the analysis is observed on the rotor blade configuration with no spar. This is followed by the rotor blade configuration with spar while the lowest bending effects on the blade configurations at various rotor speeds considered in the analysis is observed on the solid blade configurations. There is no standard to determine if the bending values will have deleterious effects that may result in failure of the wind turbine blade. However, judging from the bending values which are all less than one (1), the blade may not

obviously fail during operation. Aerodynamic loads/forces exerted by the wind on turbine rotor blades depend on blade configurations which in turn influences the blade aerodynamics. Large deflections on the blade can result in bending stresses and cause significant vibrations which consequently reduce clearance between the turbine shaft and the blade. However, with blades having the capacity to bend to some extent, advantage can be drawn from aerodynamic effects such that, the wind that gets slide over the blade results at increased area of contact, thereby, exerting more force on the blade for effective rotation and power recovery.

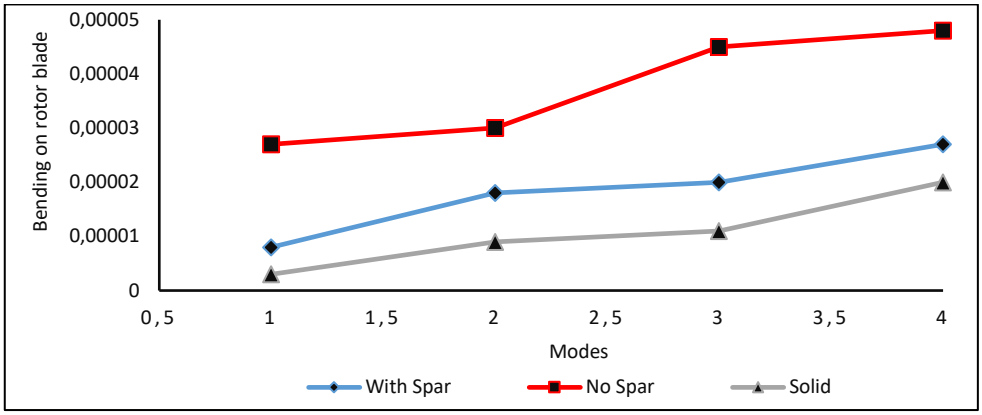

Figure 8. *Bending on Rotor Blade for Different Mode Cycles at Rotation Speed of 2m/s*

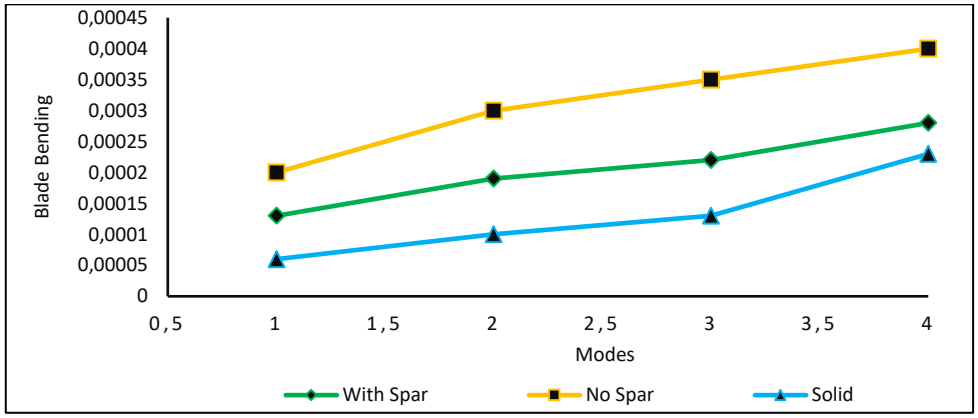

Figure 9. *Bending on Rotor Blade for Different Mode Cycles at Rotation Speed of 4m/s*

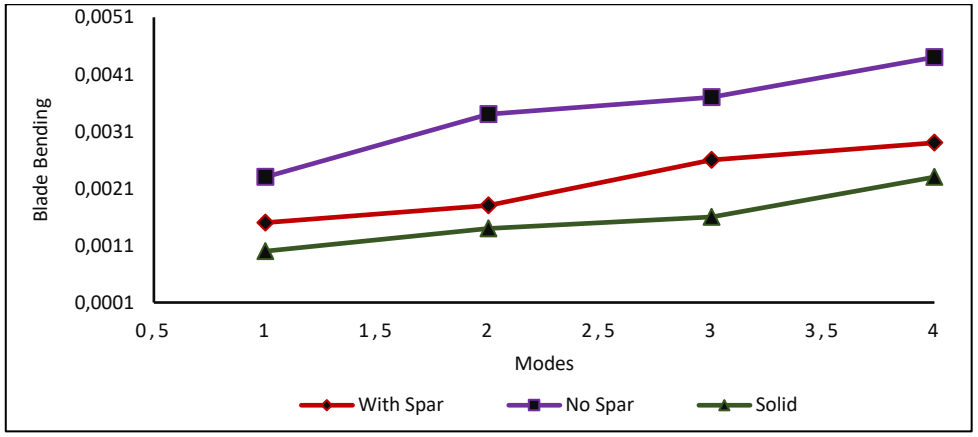

Figure 10. *Bending on Rotor Blade for Different Mode Cycles at Rotation Speed of 6m/s*

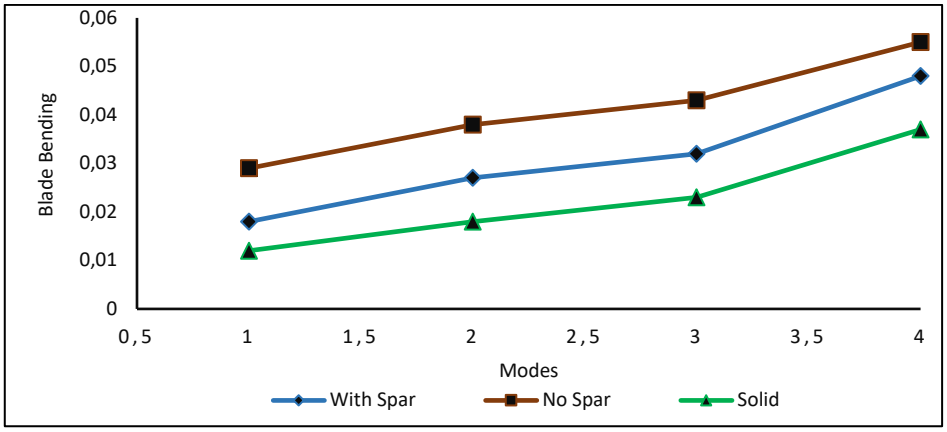

Figure 11. *Bending on Rotor Blade for Different Mode Cycles at Rotation Speed of 8m/s*

4. CONCLUSION

In this study, modal analysis was successfully carried out on horizontal axis wind turbine blade with distinct configurations under aerodynamic loading cycle. The results reveal that the aluminium solid blade is more preferred due to lower eigenvalues which offers advantage against bending stress at all rotor blade speeds as can be seen from the above analysis. The solid blade incurs additional weight but it is easy to model to specification using simple forming techniques. In actual case scenario, the additional weight can be minimized by selecting lightweight materials like the 6000 series aluminium employed in this study. Thus, for longevity and resistance against aerodynamic loads acting on wind turbine blades in duty cycle, the solid blade configuration is acclaimed to be more suitable particularly in areas with very high wind speeds.

CONFLICT OF INTEREST

There is no conflict of interest associated with the publication of this paper.

REFERENCES

Bagherpoora, T., & Xuemin, L. (2017). Structural Optimization Design of 2MW Composite wind turbine blade. Energy Procedia 105, 1226-1233.

Bhatt, P. (2009). Maximum Marks Maximum Knowledge in Physics Class X, Second Edition. Allied Publishers Private Limited, New Delhi, ISBN: 978-81-8424-444-1.

Brain, J. S., & Mark, H. R. (1999) Experimental Modal Analysis. Vibration Technology Inc, Jamestown, California, 95327.

Brøndsted, P., & Nijssen, R. (2013). Advances in Wind Turbine Blade Design and Materials. Woodhead Publishing, Oxford, UK, pp. 484.

Chaudhari, N. B. (2014). Dynamic Characteristics of Wind Turbine Blade. International Journal of Engineering Research and Technology, 3(8), 1-6.

Chen, C. P., & Kam, T. Y. (2011). Failure Analysis of Small Composite Sandwich Turbine Blade Subjected to Extreme Wind Load. Procedia Engineering, 14, 1973-1981.

Efe-Ononeme, O. E., Ikpe, A. E., & Ariavie, G. O. (2018). Modal Analysis of Conventional Gas Turbine Blade Materials (UDIMET 500 and IN738) For Industrial Applications. Journal of Engineering Technology and Applied Sciences, 3(2), 119-133.

Etuk, E. M., & Ikpe, A. E. (2020a). 3D Modelling of the Wind Flow Trajectories and Its Characteristic Effects on Horizontal Axis Wind Turbine at Different Wind Regimes. Journal of International Environmental Application and Science, 15(2), 68-80.

Etuk, E. M., Ikpe, A. E., & Adoh, U. A. (2020b). Design and Analysis of Displacement Models for Modular Horizontal Wind Turbine Blade Structure. Nigerian Journal of Technology, 39(1), 121-130.

Garolera, A. C., Madsen, S. F., Nissim, M., Myers, J. D., & Holboell, J. (2016). Lightning Damage to Wind Turbine Blades from Wind Farms in the US. IEEE Transactions on Power Delivery, 31(3), 1043-1049.

Higham, N. J., Mackey, D. S., Tisseur, F., & Garvey, S. D. (2008). Scaling, Sensitivity and Stability in the Numerical Solution of Quadratic Eigenvalue Problems. International Journal for Numerical Methods in Engineering, 73, 344-360.

Ikpe, A. E., Owunna, I., Ebunilo, P. O., & Ikpe, E. (2016a). Material Selection for High Pressure (HP) Compressor Blade of an Aircraft Engine. International Journal of Advanced Materials Research, 2(4), 59-65.

Ikpe, A. E., Owunna, I., Ebunilo, P. O., & Ikpe, E. (2016b). Material Selection for High Pressure (HP) Turbine Blade of Conventional Turbojet Engines. American Journal of Mechanical and Industrial Engineering, 1(1), 1-9.

Ikpe, A. E., Efe-Ononeme O. E., & Ariavie, G. O. (2018). Thermo-Structural Analysis of First Stage Gas Turbine Rotor Blade Materials for Optimum Service Performance. International Journal of Engineering and Applied Sciences, 10(2), 118-130.

Ikpe, A. E., Ndon, A. E., & Etuk, E. M. (2019). Response Variation of Chladni Patterns on Vibrating Elastic Plate under Electro-Mechanical Oscillation. Nigerian Journal of Technology, 38(3), 540-548.

Ivan, B., Marco, A., & Mathias, L. (2014). Physically and Geometrically Non-linear Vibrations of Thin Rectangular Plates. International Journal of Non-Linear Mechanics 58, 30-40.

Larsen, G. C., Hansen, M. H., Baumgart, A., & Carlen, I. (2002). Modal Analysis of Wind Turbine Blades. Denmark, Forsknings center Risoe, Risoe-R, 1181, ISBN: 87-550-2697-4.

Marulo, F., Petrone, G., Alessandro, V. D., & Lorenzo, E. D. (2014). Operational modal analysis on a wind turbine blade. Proceedings of ISMA2014 and USD2014, 783-798.

Mishnaevsky, L., Branner, K., Petersen, H. N., Beauson, J., McGugan, M., & Sørensen, B. F. (2017). Materials for Wind Turbine Blades: An Overview. Materials, 10(1285), 1-24.

Mouhsine, S. E., Oukassou, K., Ichenial, M. M., Kharbouch, B., & Hajraoui, A. (2018). Aerodynamics and Structural Analysis of Wind Turbine Blade. Procedia Manufacturing, 22, 747-756.

Okokpujie, I. P., Okonkwo, U. C., Bolu, C. A., Ohunakin, O. S., Agboola, M. G., & Atayero, A. A. (2020). Implementation of multi-criteria decision method for selection of suitable material for development of horizontal wind turbine blade for sustainable energy generation. Heliyon, 6, e03142.

Owunna, I., Ikpe, A. E., Satope, P., & Ikpe E. E. (2016). Experimental Modal Analysis of a Flat Plate Subjected to Vibration. American Journal of Engineering Research, 5(6), 30-37.

Pedersen, H. B., & Kristensen, O. J. D. (2003). Applied modal analysis of wind turbine blades: Modal analysis on loaded and unloaded blade, Denmark. Forsknings center Risoe, Risoe-R, 1388(7), 41-46.

Tartibu, L. K., Kilfoil, M., & Vandermerwe, A. J. (2012). Vibration Analysis of a Variable Length Blade Wind Turbine. International Journal of Advances in Engineering and Technology, 4(1), 630-639.

Taware, G. B., Mankar, S. H., Ghagare, V. B., Bharambe, G. P., & Kale, S. A. (2016). Vibration Analysis of a Small Wind Turbine Blade. International Journal of Engineering and Technology, 8(5), 2121-2126.

Soriano, L. A., Yu, W., & Rubio, J. J. (2013). Modelling and Control of Wind Turbine. Mathematical Problems in Engineering, 982597, 1-13.

Vermeer, L., Sorensen, J., & Crespo, A. (2003). Wind Turbine Wake Aerodynamics. Progress in Aerospace Sciences, 39, 467-510.

Yasuda, Y., Yokoyama, S., Minowa, M., & Satoh, T. (2012). Classification of Lightning Damage to Wind Turbine Blades. IEEE J. Trans, 7, 559-566.